1. CHARACTERISTICS OF ACCELERATOR BASED NEUTRON SOURCES

MONOENERGETIC NEUTRON PRODUCTION BY TWO-BODY REACTIONS IN THE ENERGY RANGE FROM 0.0001 TO 500 MEV

(Overview)

M. Drosg

Institute of Experimental Physics, University of Vienna, A-1090 Wien, AUSTRIA

ABSTRACT

Monoenergetic neutron sources based on two-body reactions are reviewed for neutron energies between 0.1 keV and 500 MeV. In particular the following neutron producing reactions are considered: ^{3}H(p,n)^{3}He, ^{6}Li(p,n)^{6}Be, ^{7}Li(p,n)^{7}Be, ^{9}Be(p,n)^{9}B, ^{10}Be(p,n)^{10}B, ^{10}B(p,n)^{10}C, ^{11}B(p,n)^{11}C, ^{12}C(p,n)^{12}N, ^{13}C(p,n)^{13}N, ^{14}C(p,n)^{14}N, ^{15}N(p,n)^{15}O, ^{36}Cl(p,n)^{36}Ar, ^{39}Ar(p,n)^{39}K, ^{59}Co(p,n)^{59}Ni, ^{2}H(d,n)^{3}He, ^{3}H(d,n)^{4}He, ^{7}Li(d,n)^{8}Be, ^{13}C(d,n)^{14}N, ^{15}N(d,n)^{16}O, ^{18}O(d,n)^{19}F, ^{20}Ne(d,n)^{21}Na, ^{24}Mg(d,n)^{25}Al, ^{28}Si(d,n)^{29}P and ^{32}S(d,n)^{33}Cl, using either the light or the heavy particle of the entrance channel as a projectile. In the (p,n) case the use of the heavy particle as a projectile results in a strong enhancement of the forward neutron yield due to kinematic collimation of the neutrons into a forward cone. The potential of the sources is discussed and practical aspects are stressed. It is shown that by using ^{1}H(t,n)^{3}He it should be possible to build a source of 14 MeV neutrons with an effective source strength of 10^{15} n/s which would also be useful in neutron radiotherapy.

Keywords: Neutron sources, epithermal neutrons, fast neutrons, high energy neutrons, neutron radiotherapy, neutron radiography, (p,n) reactions, (d,n) reactions, fusion, intense neutron sources

1. INTRODUCTION

Two-body reactions are a convenient and powerful way to produce monoenergetic neutrons. In most cases such sources will be accelerator based. However, there is also a (portable) electrostatically focussed plasma d-d source [1] available which is very promising for many applications.

Accelerator-based neutron production by two-body reactions does not necessarily give a pure monoenergetic neutron beam. In many cases there will be a contamination with intrinsic neutron background (other neutron lines from the excitation of non-ground-state levels or neutrons from break-up reactions) and/or with structural and room background.

Therefore the monochromaticity of a source must be viewed at with an eye on the application. Basically there are three types of applications:

a) scientific ones (physics)
b) technical ones and
c) medical ones.

In each case the demands on a monoenergetic source can differ greatly.

Up to now, mainly monoenergetic neutron sources for scientific applications have been dealt with [2-11]. By tagging the neutrons of the desired energy (e.g. by the time-of-flight method or by the associated particle method) the intrinsic background can be supressed. This type of background may then often be tolerated. The other sources of background can usually be dealt with by performing a background run and subtracting it.

Detectors in technical applications (radiography, detection of contrabands, land mine detection, applications in mining etc.[12]) will often not allow tagging, so that low intrinsic background becomes important. However, in principle, background runs are possible in many cases allowing subtraction of structural and room background.

In medical applications the situation is completely different. There the neutron beam may not contain neutrons of harmful energies (above a certain intensity limit). Obviously background runs are not an answer. On the other hand, the energy width of the primary neutron beam is of little importance allowing the use of thick targets (like in many technical applications, too). The development of the plasma port hole [13] as a nearly massless window for gas targets has helped in reducing the structural background, i.e. the amount of harmful neutrons in neutron therapy.

Although the physics of monoenergetic neutron production is independent of its application the main emphasis of this paper is laid on nonscientific applications, because the scientific angle has been dealt with in the past often and to a great extent. Reflecting the steadily increasing need of (monoenergetic) neutron sources in many fields (radiotherapy, radiography, detection of contrabands and land mines, etc.) important technical

developments have occured in recent years: portable fast neutron generators [1,14] and practicable massless windows for gas targets [13].

This paper gives an overview over neutron production by accelerators starting at epithermal energies as needed for BNCT [15] up to 500 MeV as used in some medium energy experiments. In addition, four (d,n) neutron sources are presented which could, aside from the d-D (and d-T) reaction also be used in portable accelerators, allowing monoenergetic neutron production down to 46 keV. Besides the cross section data base of two-body neutron reactions is updated and discussed.

2. GENERAL PROPERTIES OF MONOENERGETIC NEUTRON SOURCES

2.1. Monochromacity

A neutron source is considered monoenergetic when the energy spectrum consists of a single line with an energy width which is much less than the energy itself. In accelerator based sources this width is mainly determined by the target thickness. In practical applications it is usually of little importance to have a narrow energy width of the line. So the "thick target yield" of a source is of interest, rather than the differential one.

In principle, such monoenergetic neutrons can be produced by two-body reactions. However, a practial source will not only produce these foreground (primary) neutrons, but also "background" neutrons, either from beam interactions in the accelerator and target structure or from interactions of the primary neutrons with the room structures (beam connected room background, inscattered neutrons). This background depends, of course, strongly on the "hardware" in use and not on the source reaction itself.

In addition, there may be a source intrinsic background of (secondary) neutrons which cannot be distinguished from foreground neutrons. This background either consists of lines of other two-body reactions in the target, of an energy distribution of more-body reactions (break-up) or of the satellite line as a result of kinematic collimation.

2.1.1 Kinematic collimation

If in a two-body reaction the velocity of the center-of-mass (c.m.) is larger than the c.m. velocity of the particle that is emitted at 180° c.m., there will be two lines in the 0° energy spectrum: the primary line corresponding to 0° c.m. emission and the secondary, satellite line from 180° c.m. Such two-line neutron spectra occur in endothermic reactions either in a narrow energy range above the threshold or, if the projectile is heavier than the target nucleus, over the entire energy range above the threshold. Consequently the neutron emission is compressed into a forward cone with two neutron groups at each angle inside the cone.

This confinement of the neutrons into a forward cone is very beneficial for the following reasons:

a) minimum room background
b) simplified shielding (it makes shadow bars at back angles obsolete)
c) strongly enhanced laboratory cross section of the 0° c.m. line
d) reduced laboratory cross section of the 180° c.m. satellite neutron line. Thus the satellite line may be disregarded in many applications. This is especially true at high enough projectile energies. There not only the cross section but also the energy of neutrons from 180° in c.m. becomes much smaller than those of neutrons from 0° in c.m. making them an even smaller disturbance.

At a projectile energy E_p the (half) opening angle Θ of the forward cone is given nonrelativistically by

$$\sin^2 \Theta = (1 - E_{th}/E_p)\, M_2M_4/M_1M_3$$

The masses M_i are those of the projectile, the target, the neutron and the residual nucleus resp., E_{th} is the threshold energy of the reaction.

For a given neutron energy E_n at 0° the following (nonrelativistic) relation holds

$$(1 + \sin \Theta)^2 = (1+M_2/M_1)(1+M_4/M_3).E_n/E_p$$

Therefore, for a desired neutron energy the cone will become narrow with

a) M_2 small,
b) M_4 small and
c) $E_p >> E_n$, i.e. for reactions with large negative Q-values.

2.2 Intensity

Obviously, regular applications of a neutron source require that one individual application should defintely last shorter than about 10^3 s. The shorter the better. Therefore, intensity of a source is more important in practical than in scientific applications.

The yield of neutrons of the desired energy from an accelerator based monoenergetic source depends on
- the charged particle beam intensity,
- the target thickness,
- the differential cross section of the reaction
- the specific energy loss in the target material.

The target thickness is determined by the required monochromaticity and needs no further discussion.

The charged particle beam intensity is limited on the one hand by the capability of the accelerator, on the other hand by the maximum allowed heat load of the target because the power dissipated in the target depends on beam intensity and energy loss in the target.

Therefore, it is convenient to compare intensities of monoenergetic neutron sources by their (energy dependent) specific yield which is usually given in the units of neutrons/(sr.μC.MeV), as has been pointed out before [16]. Such a comparison does not take the target power into account. Therefore for intense sources a comparison should rather be based on power (current x voltage).

To achieve a high specific yield it is necessary to have both a high neutron production cross section and a small energy loss of the projectile in the target.

2.2.1 Differential cross sections

The differential neutron producing cross section is one main property of a two-body neutron source. Usually only neutron emission at an angle of 0° with respect to the charged particle beam is considered.

Placing the sample at 0° has the following advantages:

- The neutron yield is usually forward peaked.
- Neutrons emitted at 0° have the highest energy. Therefore there are no source connected background neutrons which have higher energy.
- Neutrons emitted at 0° are certainly unpolarized.
- At 0° the angular dependence of both the neutron energy and of the neutron yield on the angle is comparatively small.

For this reason monoenergetic neutron sources are usually compared by their 0° yield, as will be done here, too.

However, as shown in Fig. 1 for 0.3 MeV neutrons, maximum monoenergetic yield at this energy is not necessarily obtained at 0°. For p-^{7}Li the yield at 70° is about thrice that at 0°! Such two-dimensional yield information can be found for the basic reactions in graphical form [4] or may be obtained for a large variety of reactions by way of a computer program [17].

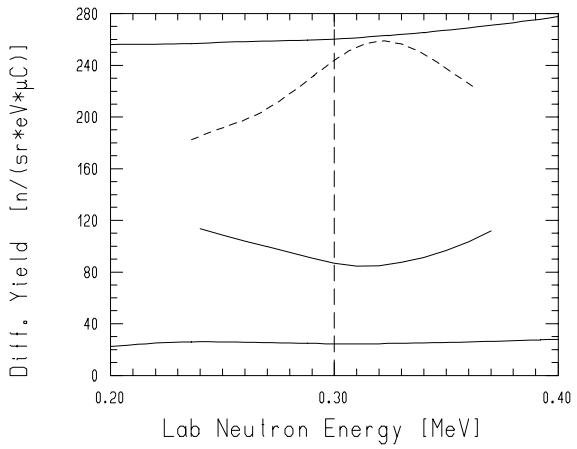

FIG. 1. Specific neutron yield for the product-ion of 0.3 MeV neutrons. Bottom to top: p-^{11}B (0°), p-^{7}Li (0°), p-^{7}Li(70°), p-^{3}H(0°)

2.2.2 Electronic stopping power

The beam particles hitting a target get slowed down by interactions with the electrons (straggling) until they are in thermal equilibrium with their surroundings. As a consequence one gets a white neutron spectrum if the projectiles are completely stopped in the target, even if all nuclear reactions were two-body reactions. Therefore, a target may only be as thick as the required neutron energy width allows. For a given target thickness (= neutron energy width) there will be the more nuclear interactions (i.e. produced neutrons) the lower the electronic stopping cross section is (compared to the nuclear cross section).

Consequently, reactions with hydrogen targets, which have the lowest electronic stopping power, give the highest neutron yield. Thus most useful monoenergetic neutron reactions are of the form ^{k}H+A=n+B+Q (k=1,2,3), where the Q-value can be

- positive: (d,n) or
- negative: (p,n).

2.2.2.1 Reactions with hydrogen isotopes

These include the "traditional" sources where ions of the hydrogen isotopes are accelerated. With the advent of heavy ion accelerators the inverse reaction became also available. There the projectile is heavier than the target resulting in a kinematically collimated neutron beam (see 2.1.1).

The traditional sources have been utilized for such a long time that already the review article of Brolley and Fowler in the year 1958 [2] covers at least qualitatively most of today's knowledge in this field. Modern developments are covered in several recent review articles [3 - 11]. Moreover, since 1987 there has been a (regularly updated) code available [18] that allows the calculation of kinematic properties and differential neutron yields of (presently) 43 neutron sources based on two-body reactions with at least one hydrogen nucleus.

Not included in this code and in this paper are three (p,n) reactions which have a very narrow monoenergetic range only and which are mostly used for detector calibration in the keV range:

$^{45}Sc(p,n)^{45}Ti$ [3,7]
$^{51}V(p,n)^{51}Cr$ [3,6,7] and
$^{57}Fe(p,n)^{57}Co$ [3].

2.2.3 Target construction

The ideal target is isotopically pure and self-supporting. If other constituents are present, the specific neutron yield for a given energy loss of the charged particle beam in the (active) portion of the target is lower because of the lower areal density of the target material reducing the yield itself. In addition, there will be additional (energy) straggling from the additive, so that (in a specific application) these additives will increase the energy spread reducing the specific neutron yield further.

2.2.3.1 Gas targets

Many monoenergetic neutron sources use an isotope of hydrogen as target medium. So gas targets are necessary to achieve isotopically pure targets (disregarding cryogenic liquid targets). The container of the target medium is usually a (thin walled) cell of stainless steel, with an entrance window towards the accelerator vacuum. At the other end there is a solid disc as a beam stop which collects the charged particle beam. The alternative, to use an exit window as well and to bend the beam by a clearing magnet into a beam dump is seldom used although the structural background can be much reduced this way.

A detailed description of target technology has been given before, e.g. [3] and [9]. Since then there has been a very important new development: practically massfree gas containment by plasma port holes [13] which is beneficial at least in two ways:

1) reduced structural background and
2) reduced total power dissipation in the target.

In addition, there is practically no energy degradation and straggling in the entrance window resulting in sharper edges of the neutron distribution. This new technology appears to be by far superior to previous windowless target designs [19 - 21].

2.2.3.2 Solid targets

In many cases (e.g. for p-^{7}Li and p-^{11}B) isotopically pure solid targets are possible. Usually they have a backing with good thermal conductivity (gold, silver, copper, aluminum, tantalum, tungsten) which serves as a beamstop and allows beam power removal by means of an air jet or a water spray.

In addition, there exist solid hydrogen targets (hydrides of Ti, Zr, Er, Sc or Y). Of these titanium hydride is known best. Typically, titanium is impregnated with 1.5 hydrogen atoms per titanium atom. The advantage of solid hydrogen targets is the absence of a window which results in much better energy resolution if low energy beams are used like in the d-T case. The main disadvantage is the strongly reduced specific yield (by about an order of magnitude) because of the other constituent in the active volume of the target. Whether the newly developed plasma port hole [13] which would provide an ideal massless window for the low energy d-T reaction will actually be used in connection with a tritium target remains to be seen.

2.3 Kinematic and nuclear structure properties

2.3.1 (p,n) Reactions and inverse (p,n) reactions

By inverting a (p,n) reaction the monoenergetic neutron energy range at 0°, i.e. the maximum monoenergetic neutron energy is much increased because of the much higher projectile energy employed to get the same c.m. energy which results in a higher velocity of the c.m. motion. The neutrons are kinematically collimated into a forward cone (see 2.1.1). The much higher 0° yield, the small room background and the simplified shielding make these "inverse" sources stand out.

However, as discussed before (2.1.1), such sources are not truly monoenergetic but have two-line spectra. In many applications this does not matter.

Such kinematic collimation and two-line spectra are also present in a small energy range of regular (p,n) reactions at and above threshold. Table 1 summarizes relevant energy data for these double valued regions.

TABLE 1. RELEVANT ENERGIES IN THE DOUBLE-VALUED ENERGY REGION OF SEVERAL (P,N) REACTIONS

Reaction Type	Q-value [MeV]	Proj. Energy Range [MeV]		Neutron Energy Range [keV]		E_{n0max} [MeV]
		from:	to:	from:	to:	
$^{3}H(p,n_0)^{3}He$	0.764	1.0191	1.1473	64.	288.	7.585
$^{6}Li(p,n_0)^{6}Be$	-5.071	5.9223	6.0940	122.	503.	2.558
$^{7}Li(p,n_0)^{7}Be$	-1.644	1.8807	1.9204	29.7	121.	0.651
$^{7}Li(p,n_1)^{7}Be*$	-2.074	2.3714	2.4215	37.5	153.	2.015
$^{9}Be(p,n_0)^{9}B$	-1.851	2.0578	2.0840	21.8	84.5	1.951
$^{10}Be(p,n_0)^{10}B$	-0.227	0.2496	0.2522	2.1	8.4	1.176
$^{10}B(p,n_0)^{10}C$	-4.431	4.8774	4.9275	41.	165.	4.055
$^{11}B(p,n_0)^{11}C$	-2.765	3.0187	3.0443	21.3	85.8	2.388
$^{12}C(p,n_0)^{12}N$	-18.121	19.657	19.798	119.	479.	1.678
$^{13}C(p,n_0)^{13}N$	-3.003	3.2363	3.2559	16.8	67.5	2.278
$^{14}C(p,n_0)^{14}N$	-0.626	0.6714	0.6749	3.2	12.2	2.415
$^{15}N(p,n_0)^{15}O$	-3.537	3.7748	3.7920	15.8	60.3	5.742
$^{36}Cl(p,n_0)^{36}Ar$	-0.076	0.07757	0.07763	0.1	0.3	2.028
$^{39}Ar(p,n_0)^{39}K$	-0.219	0.2248	0.2250	0.2	0.6	2.593
$^{59}Co(p,n_0)^{59}Ni$	-1.858	1.8897	1.8902	0.5	2.1	0.33

2.3.2 (d,n) and inverse (d,n) reactions

Among the (exothermic) (d,n) reactions only d-D and d-T have been used frequently. These two reactions have a rather wide monoenergetic range (see Table 2, E_{n0max}). With the advent of accelerator based portable neutron sources [14] (accelerators with a low maximum acceleration voltage and consequently a small energy range) an interest in additional endothermic reactions has arisen to make additional monoenergetic neutron energies available.

There are four more single line (d,n) neutron reactions available, namely $^{20}Ne(d,n_0)^{21}Na$, $^{24}Mg(d,n_0)^{25}Al$, $^{28}Si(d,n_0)^{29}P$ and $^{32}S(d,n_0)^{33}Cl$, that could provide additional neutron energies for low energy accelerators. However, at present no data on the neutron yield of these sources at low beam energy are available, so that it is unclear whether they are useful at all.

In an effort to get (alternate) neutron sources for the gap region (below 14 MeV) d-^{7}Li, d-^{11}B, d-^{13}C and d-^{15}N have been considered because of their high Q-values, despite their multi-line spectra (see Table 2). These four sources have minimum neutron energies at 0° (E_{n0min}) of 13.338, 12.668, 4.986 and 9.312 MeV, respectively. Because of their multi-line nature the energy separation (E_{separ}) of the primary, the highest energy line from the next line, becomes important. As will be shown later (4.2) their 0° specific yield is so low that their use is not only limited by these additional neutron lines.

TABLE 2. SELECTED NUCLEAR AND KINEMATIC PROPERTIES OF SEVERAL (d,n) AND INVERSE (d,n) REACTIONS. E_{n0max} GIVES THE UPPER LIMIT OF THE MONOENERGETIC ENERGY RANGE.

Reaction Type	Q-value [MeV]	E_{n0min} [MeV]	E_{separ} [MeV]	Nr.lines at E_d=0	E_{n0max} [MeV]	E_{n0max} [MeV]
					(d,n)	inv.(d,n)
^{2}H(d,n)^{3}He	3.269	2.449	-	1	7.706	7.706
^{3}H(d,n)^{4}He	17.589	14.029	-	1	20.461	23.006
^{20}Ne(d,n_0)^{21}Na	0.206	0.197	-	1	0.344	0.644
^{24}Mg(d,n_0)^{25}Al	0.046	0.044	-	1	0.483	1.192
^{28}Si(d,n_0)^{29}P	0.522	0.505	-	1	1.444	3.208
^{32}S(d,n_0)^{33}Cl	0.050	0.049	-	1	0.855	2.207
^{7}Li(d,n_0)^{8}Be	15.030	13.338	2.696	3	16.549	21.461
^{11}B(d,n_0)^{12}C	13.732	12.663	4.092	10	13.499	15.923
^{13}C(d,n_0)^{14}N	5.326	4.968	2.157	5	5.597	7.307
^{15}N(d,n_0)^{16}O	9.902	9.312	5.690	8	10.118	12.741

By exchanging projectile and target nucleus the maximum monoenergetic neutron energy can be increased (see Table 2, last column), like in the (p,n) cases. However, the minimum energy (at zero projectile energy!) stays the same. In special cases, like for ^{3}H(d,n)^{4}He there are additional advantages of such an inversion (see 3.3.4.1).

3. PREDICTIONS OF MONOENERGETIC NEUTRON SOURCE PROPERTIES

Since 1987 a computer code package originally called DROSG-87 has been available to calculate the salient properties (laboratory and center-of-mass angles, cross sections, energies, yields) for neutron sources based on two-body reactions [18]. It was issued as a compendium [4] and is distributed free of charge by the Nuclear Data Section of IAEA in Vienna, Austria. This package is updated frequently, its latest published version [17] is called DROSG-96.

3.1. Differential neutron yields

The interactive and self explaining program NEUYIE of the package DROSG-96 calculates neutron energies and differential cross sections for monoenergetic neutron sources from internal tables of the Legendre coefficients. For isotopic pure targets it also can calculate the neutron yield using energy loss tables. The main menue of the latest update of this program is shown in Table 3.

TABLE 3. MAIN MENUE OF THE COMPUTER CODE NEUYIE.

ID	Reaction type	Remarks	E_{n0max}	X-section range [MeV]
1	$^{3}H(p,n)^{3}He$	Isotopically pure target	7.585	1.0191-32.80/318.
101		T_2O target(ice)		
2	$^{2}H(d,n)^{3}He$	isotopically pure target	7.706	0.02 - 39.80/85.
201		heavy water target		
3	$^{1}H(t,n)^{3}He$	isotopically pure target	17.639	3.051 - 98.19
301		water target(ice)		
302		octane target		
4	$^{3}H(d,n)^{4}He$	isotopically pure target	20.461	0.01 - 40.00/400.
5	$^{2}H(t,n)^{4}He$	isotopically pure target	23.006	0.015- 59.9/599.
501		heavy water target(ice)		
7	$^{7}Li(p,n_0)^{7}Be$		0.650	1.8807-7.00/494.
8	$^{1}H(^{7}Li,n_0)^{7}Be$		3.842	13.097- 48.745
9	$^{7}Li(p,n_1)^{7}Be*$	(0.429 MeV level)	1.557	2.40 - 7.00/20.
10	$^{1}H(^{7}Li,n_1)^{7}Be*$	(0.429 MeV level)	7.231	16.713 - 48.745
11	$^{11}B(p,n_0)^{11}C$		2.388	3.020/3.5 - 5.49/26.
12	$^{1}H(^{11}B,n_0)^{11}C$		11.880	33.-59.989/284.1
13	$^{13}C(p,n_0)^{13}N$		2.278	3.239 - 12.86/30.6
14	$^{1}H(^{13}C,n_0)^{13}N$		12.175	41.803/112.28-165.97
15	$^{15}N(p,n_0)^{15}O$		5.742	3.94 - 15.62
16	$^{1}H(^{15}N,n_0)^{15}O$		25.726	58.659 -232.549
17	$^{6}Li(p,n_0)^{6}Be$	isotropic approximation	1.172	6.00 - 7.874/200.
18	$^{9}Be(p,n_0)^{9}B$		-	2.20 - 30.0
19	$^{10}B(p,n_0)^{10}C$	isotropic approximation	4.055	4.94 - 8.571/17.1
20	$^{12}C(p,n_0)^{12}N$	zero degree only	1.200	25.8
21	$^{14}C(p,n_0)^{14}N$	isotropic approximation	2.522	0.6714 - 3.151/20.67
22	$^{1}H(^{14}C,n_0)^{14}N$	isotropic approximation	9.782	9.332 - 3.795/287.2
23	$^{10}Be(p,n_0)^{10}B$	isotropic approximation	0.310	0.251 - 1.040/20.247
24	$^{1}H(^{10}Be,n_0)^{10}B$	isotropic approximation	3.012	2.495 - 10.337/201.2
25	$^{36}Cl(p,n)^{36}Ar$	isotropic approximation	2.028	0.878 - 2.103
26	$^{1}H(^{36}Cl,n)^{36}Ar$	isotropic approximation	7.826	31.35 - 75.08
27	$^{39}Ar(p,n_0)^{39}K$	isotropic approximation	2.593	1.225 - 1.300/20.224
28	$^{1}H(^{39}Ar,n_0)^{39}K$	isotropic approximation	10.279	47.367 - 50.28/782.1
29	$^{59}Co(p,n)^{59}Ni$	isotropic approximation	0.363	1.8897 - 2.240/11.89

30	$^{1}H(^{59}Co,n)^{59}Ni$	isotropic approximation	4.198	110.534 - 131./695.5
31	$^{7}Li(d,n)^{8}Be$	isotropic approximation	>=3 lv	0.01 - 10.957
32	$^{2}H(^{7}Li,n)^{8}Be$	isotropic approximation	>=3 lv	0.035 - 38.5
33	$^{11}B(d,n)^{12}C$	isotropic approximation	>=10 lv	0.411 - 2.513/5.564
34	$^{2}H(^{11}B,n)^{12}C$	isotropic approximation	>=10 lv	2.247 - 13.82/30.6
35	$^{13}C(d,n)^{14}N$	isotropic approximation	>=5 lv	0.312 - 3.568
36	$^{2}H(^{13}C,n)^{14}N$	isotropic approximation	>=5 lv	2.028 - 23.04
37	$^{15}N(d,n)^{16}O$	isotropic approximation	>=8 lv	2.13E-4 - 5.979/10.1
38	$^{2}H(^{15}N,n)^{16}O$	isotropic approximation	>=8 lv	0.0016 - 44.53/75.2
39	$^{18}O(d,n)^{19}F$	isotropic approximation	>10 lv	0.975 - 2.204/14.696

E_{n0max} gives the upper limit of the mono-energetic energy range except for the multiline (d,n) reactions where the maximum numbers of neutron lines due to excited levels at E_d=0 MeV is given. An alternate upper limit of the cross section range indicates a higher energy limit just for the 0° cross section.

3.1.1 Kinematic calculations

The kinematic properties are calculated with the 1995 [22] (nuclear) masses using relativistic expressions. In most cases (not near thresholds) the mass uncertainty can be disregarded. It is assumed that the interacting nuclei are completely stripped which need not be true for a given situation.

3.1.2 Cross section data base

There are two classes of cross section data:

a) Complete angular distributions of differential cross sections (in some energy range) for: $^{3}H(p,n)^{3}He$, $^{2}H(d,n)^{3}He$, $^{3}H(d,n)^{4}He$, $^{7}Li(p,n_0)^{7}Be$, $^{7}Li(p,n_1)^{7}Be$*, $^{9}Be(p,n_0)^{9}B$, $^{11}B(p,n_0)^{11}C$, $^{13}C(p,n_0)^{13}N$ and $^{15}N(p,n_0)^{15}O$

b) Differential cross sections at 0° and/or 180° (In some cases just isotropic approximation from integrated cross sections) for: $^{6}Li(p,n_0)^{6}Be$, $^{10}Be(p,n_0)^{10}B$, $^{10}B(p,n_0)^{10}C$, $^{14}C(p,n_0)^{14}N$, $^{36}Cl(p,n)^{36}Ar$, $^{39}Ar(p,n_0)^{39}K$, $^{59}Co(p,n)^{59}Ni$, $^{7}Li(d,n)^{8}Be$, $^{11}B(d,n)^{12}C$, $^{13}C(d,n)^{14}N$, $^{15}N(d,n)^{16}O$ and $^{18}O(d,n)^{19}F$.

Often the "isotropic approximation" of the differential cross sections was obtained from the corresponding time reversed (n,p_0) or (n,d_0) integrated cross sections as found in the evaluated neutron data files (e.g. ENDF/B-6) by detailed balance calculation. Especially in those cases, where (n,p) or (n,d) instead of (n,p_0) or (n,d_0) resp., had to be used, only a crude estimate is obtained.

Thus the accuracy of the differential cross section data base differs from case to case. Usually, the source of the data is given at the end of each data file, and in special cases also an estimate of the uncertainty.

Only p-T, d-D and d-T are based on measurements and evaluations of this author, some other data bases, like that of p-^{7}Li, are partially based on (unpublished) own evaluations. Chiefly, the error discussion for these reactions and for p-^{7}Li as given in [4] is still valid, even if the cross section data have changed since then.

The tabulated data for each reaction are in a file of its own so that anybody could substitute them by (hopefully better) data of his own.

3.1.3 Yield determination

For each energy and angle differential yields are calculated for such a target thickness that at 0° the neutron energy spread is 10 keV. The electronic stopping power calculation is usually based on data of Ziegler [23] unless shown otherwise at the end of each file. Using the values of Ziegler has proven to be the best in several cases.

For energies which are moderately higher than the low energy maximum of the stopping power the solutions of different authors differ by typically 5 to 10%. At low energies the uncertainty in the energy loss can be comparatively large.

The tabulated energy loss data for each material are also in files of their own so that anybody could substitute them by (hopefully better) data of his own.

3.2 Thick target neutron yields

The energy width of "monoenergetic" sources for applied purposes will usually be wide. Therefore, the quantity of interest is the thick target yield of that source. The interactive and selfexplaining program WHIYIE of the same package DROSG-96 allows the calculation of thick target neutron spectra and yields at any angle and energy. The main menue is identical with that of NEUYIE and is shown in Table 3.

3.2.1 Thick target yields near threshold

For kinematically collimated neutron beams the opening angle becomes very small close to threshold, i.e. the beam is very narrow. This has two consequences:

a) The shape of a thick target yield curve in the double-valued energy region depends on the acceptance angle of the detector because the narrow beam does not necessarily

illuminate all of the detector. This effect is shown in Fig. 2 for the case of $^{7}Li(p,n_0)^{7}Be$ with acceptance angles of 2° and 5°. (A differential yield curve - with 0° acceptance angle - will show infinities at the boundary angles of the neutron cone.)

b) The shape also depends on effects (angular straggling, elastic proton and neutron scattering) that change the outgoing neutron direction with regard to the incoming beam direction. So a narrow neutron beam can be deflected so much that it does not hit the detector at all. Therefore it is not surprising that the maximum of an actually measured 0° thick-target yield curve [24] is flatter and less pronounced than shown in Fig. 2.

3.2.1.1 $^{7}Li(p,n_0)^{7}Be$

Recently there has been some interest in near threshold thick target yields of p-^{7}Li for BNCT applications [25]. Relevant predictions of DROSG-96 for them are given in Fig. 2.

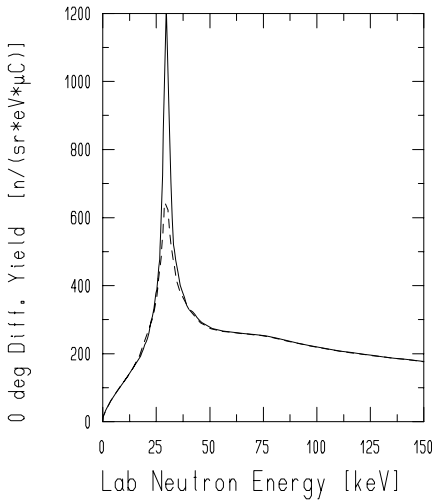

FIG. 2. Thick-target yields of $^{7}Li(p,n_0)^{7}Be$ near threshold for a 2° opening angle (full curve) and a 5° opening angle (dashed)

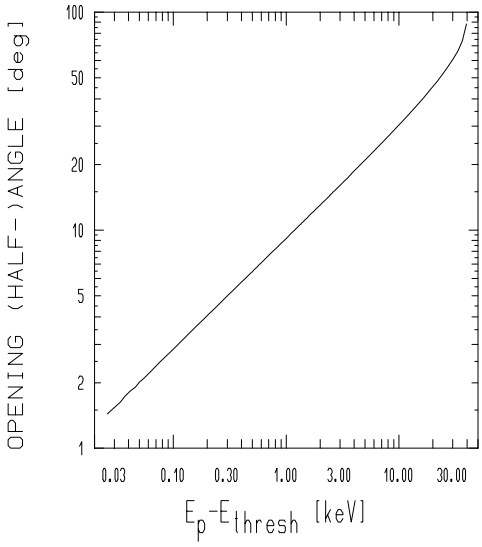

FIG. 3 Half-opening angle of the cones of the $^{7}Li(p,n_0)^{7}Be$ reaction in dependence on the beam energy minus threshold energy.

3.3 Selected reactions: description and a cross section update

3.3.1 (p,n) reactions
3.3.1.1 $^{3}H(p,n)^{3}He$

Between 64 und 288 keV neutron energy (at 0°) the neutrons are kinematically collimated. Consequently such neutron spectra have two lines. Beyond 0.288 MeV clean single line neutron spectra are obtained up to 7.585 MeV where triton break-up sets in. However, the intrinsic background above the break-up threshold is not severe (its

contribution to the total spectrum is only 23 % at 14 MeV) so that this source has been used in special applications even above 14 MeV [26] taking advantage of the about thirtyfold higher specific yield than that of the usual 14 MeV (d-T) generator.

This source is the most desirable source for nearly all energies, even up to 300 MeV [8,27] (see 4.3), if the background from the triton break-up can be tolerated.

Below about 2 (or 3) MeV neutron energy solid targets (2.2.3.2) are used for improved resolution with the consequence of a reduced yield. Recently, necessary corrections when using such solid targets have been investigated thoroughly [28].

With regard to data accuracy there has been a breakthrough at lower energies. The shape of the integrated cross section curve up to 4.5 MeV [29] agrees below 1.55 MeV perfectly with an independent R-matrix analysis [30] which incorporated recent polarization data [31]. The required scale adjustment of 2.0% is well within the 5 % scale error of the new data. This new work excels by its careful energy determination which is crucial in this energy range, as has been pointed out before [32]. Above 2.9 MeV the shape agrees perfectly with the tabulated data of DROSG-96. So in version 2.0 of DROSG-96 only data below 2.9 MeV had to be modified. The new data base uses Hale's differential cross section data [30] up to 1.55 MeV and the shape of Brune's integrated data [29] further up to 2.9 MeV. This new solution is shown in Fig. 4 by the full line, the old one by short dashes.

The advantages of p-T over the popular d-D reaction has been discussed comprehensively before [9]. However, the radioactivity of the target often precludes its use.

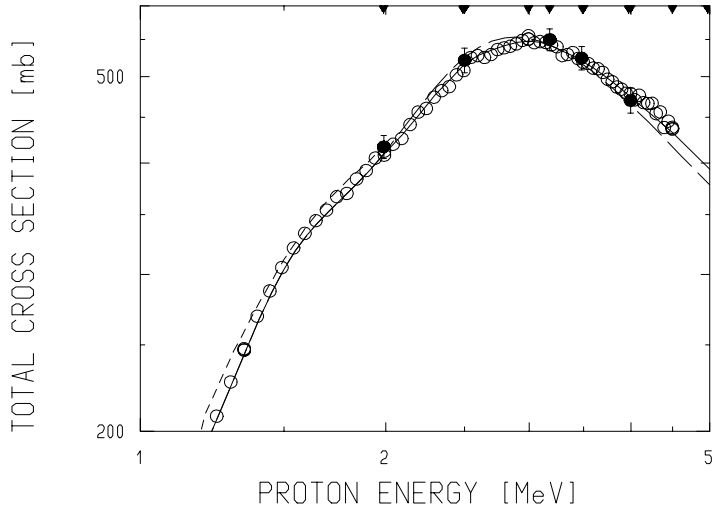

FIG.4. Reaction cross sections of $^{3}H(p,n)^{3}He$. Open circles are data of Brune [29] multiplied by 1.031, full circles are old data by this author. See text for discussion.

3.3.1.2 $^{7}Li(p,n_0)^{7}Be$

This is the most common source at lower energies, especially below 0.7 MeV. Between 29.7 and 121 keV neutron energy (at 0°) the neutrons are kinematically collimated. Consequently such spectra have two lines. Beyond 0.121 MeV clean single line neutron spectra are obtained up to 0.650 MeV. At that energy the 0.429 MeV level of ^{7}Be gets excited so that three-, and above 0.703 MeV two-line spectra are present up to 2.015 MeV neutron energy, where ^{7}Li break-up with neutron emission sets in. The intensity of the second neutron group is typically less than 10 % [33] so that it can be tolerated in some applications. At about 6 MeV neutron energy already 40 % of all neutrons are continuum neutrons. p-^{7}Li has been used above the break-up threshold applying calculated corrections for the effect of the break-up continuum [34].

The advantages of the p-^{7}Li source are [9]:

a. Small kinematic energy spread
b. Reasonable neutron intensity
c. Relatively high projectile energy which gives e.g. better time resolution in time-of-flight experiments
d. Simple target production: Usually targets consist of lithium metal evaporated on a tantalum [34 - 36], silver or tungsten backing. Even natural lithium which contains 7.5 % ^{6}Li can be used. (The (p,n) threshold of ^{6}Li at 5.9223 MeV is outside the useful lower energy range of the p-^{7}Li reaction). Although the handling of the compound LiF which is also used as a target material is much easier, metallic Li is better because its specific neutron yield is three times as large.

That the handling of metallic Li must be done very carefully was recently demonstrated. A paper in the year 1996 [37] suggested that the integrated thick target yields below 1.99 MeV as calculated by the code WHIYIE of DROSG-96 are high by about 50 %.

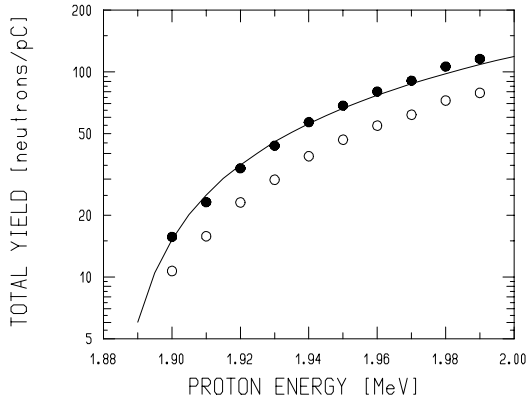

FIG. 5. Total neutron yield from the p-^{7}Li reaction using lithium metal as a target. Full line: prediction of DROSG-96, full dots: data of [37] multiplied with 1.466.

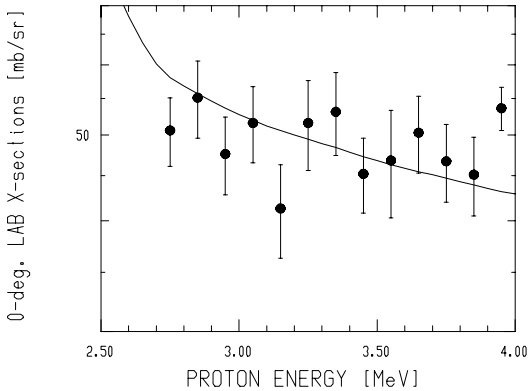

FIG. 6. Experimental data [39] and predictions of the code NEUYIE of DROSG-96.

However, this paper has an internal inconsistency of 46.6% if the yield of metal targets is compared with that of LiF and Li_2O. After raising the measured data by that amount a rather good agreement is obtained with the calculated prediction (see Fig.5). The reason for this discrepancy was traced to inadequate handling of the metal target so that hydroxide was present [38].

In another recent experiment the 0° differential cross sections between 2.7 and 4.0 MeV proton energy were measured [39]. These data agree within their uncertainties so well with the predictions of the DROSG-96 that they do not suggest any change of the data base in this energy range (see Fig. 6).

For a discussion of the peculiarities of the thick target yield in the two line region near threshold see 3.2.1.

This source is also a very popular source for high energies, even up to 500 MeV (see Sect.4.3).

3.3.1.3 $^{11}B(p,n_0)^{11}C$

Between 21.3 und 85.8 keV neutron energy (at 0°) the neutrons are kinematically collimated. Consequently such spectra have two lines. Beyond 0.0858 MeV clean single line neutron spectra are obtained up to 2.388 MeV. At that energy the 2.000 MeV level of ^{11}C gets excited so that the spectrum gets contaminated with two resp. one additional line, until at 4.941 MeV neutron energy ^{11}B break-up with neutron emission sets in. This source has not been much in use, although compared to the popular p-^{7}Li reaction it has several advantages:

a) a smaller minimum energy
b.) a smaller kinematic energy spread
c) a better intrinsic energy resolution (higher threshold) and, above all,
d) a much wider monoenergetic energy range.

However, the specific yield is similar to that of p-T with solid targets, i.e. up to an order of magnitude lower than that of p-^{7}Li. Furthermore, boron-11 targets are more difficult to produce than lithium-7 targets.

3.3.2 Inverse (p,n) reactions

3.3.2.1 $^{1}H(t,n)^{3}He$

This kinematically collimated source is monoenergetic between 0.573 and 17.639 MeV neutron energy corresponding to triton energies between 3.0508 and 25.010 MeV. Taking the satellite line into account one gets an effective monochromaticity which increases with increasing primary energy (e.g. at a primary energy of 14 MeV the satellite

line has only an energy of 0.024 MeV and its intensity is lower by a factor of 2700). In the gap region the specific yield of this source surpasses that of any other by an order of magnitude. The primary neutrons are confined into a forward cone (with a total opening angle of 130° at 14 MeV) with all its advantages (see 2.1.1).

Routinely, this source has been used only at Los Alamos for neutron energies up to 13 MeV, either bunched with about 0.6 μA average current [40 - 42] or with up to 10 μA DC current giving a source intensity of 10^{11} n $sr^{-1}s^{-1}$ [43]. The capability of this source reaction for intense monoenergetic and/or white applications is unsurpassed (see 4.4).

To obtain energies between 573 and 19.1 keV the second neutron group (the satelllite line) may be used. This has been demonstrated in an experiment for which low energy neutrons down to 50 keV [44] were provided by this source.

Fig.7 gives an example (0°, 7.07 MeV triton energy) of the energy spectrum (after time-of-flight to energy conversion and correction for the energy dependence of the detection efficiency) showing (from right to left) the onset of the neutron background (from the triton interactions in the target structure), the high-energy monoenergetic neutron line at 4.1 MeV and the low-energy monoenergetic neutron line at 80 keV.

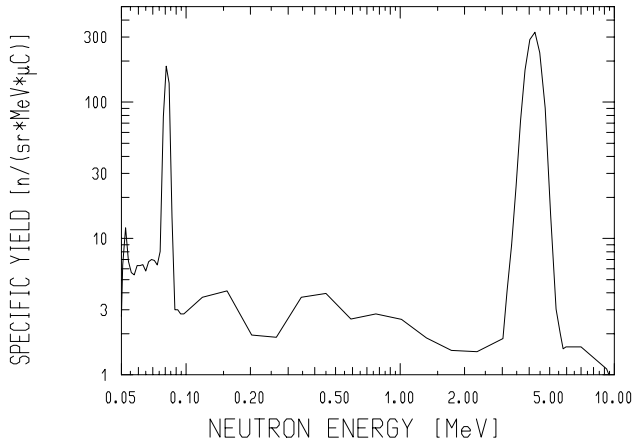

FIG. 7 Neutron energy spectrum produced by the $^{1}H(t,n)^{3}He$ reaction at 0° with 7.1 MeV tritons.

The main disadvantage of this source which prevented its general use up to now is the concern about the radioactivity of the triton beam. Another disadvantage was, until recently, the rather high structural background from the triton interaction with the gas cell, requiring a "gas-out" run for background subtraction. However, the new development of a plasma porthole [13] to contain the gas in the cell will make such background runs unnecessary.

In low energy applications also the background stemming from the rather intense high-energy (primary) line must be considered which, obviously, cannot be corrected for by a "gas-out" run.

3.3.2.2 $^{1}H(^{7}Li,n_0)^{7}Be$

This kinematically collimated neutron source is monoenergetic between 1.439 and 3.846 MeV (disregarding the inevitable satellite peak). Up to 8.19 MeV when break-up sets in there is a two-line (actually four-line) region (from the 0.429 MeV state of ^{7}Be) [45].

This reaction has been experimentally investigated at Duke [46]. From these measurements it can be concluded that this source can have significant advantages when used near the threshold (for neutron energies below about 1.7 MeV), not only because of the high yield but more so because of the narrow collimation (total opening angle <10°). In addition only a low gamma ray flux was observed.

At the other energies the specific yield is moderate so that the disadvantage of a satellite peak (which, in this case, cannot be neglected, neither in energy nor in intensity) will usually override the advantage of the kinematic collimation.

3.3.2.3 $1H(^{11}B,n_0)^{11}C$

With this kinematically collimated source monoenergetic neutrons between 2.536 and 11.880 MeV can be produced. Beyond that energy there is a two- (four-) line spectrum.

This source was used for the first time at the tandem of JAERI in Tokai [47]. Taking advantage of the cross section maximum at 11.4 MeV in the middle of the "gap", several experiments have been performed at this energy. At 0° a differential source strength of 1.10^{7} n $sr^{-1}s^{-1}$ of 11.4 MeV was obtained with a basic energy resolution of 6.8 % (0.1 e mA beam of ^{7}Li, 4 ns burst width). In the DC mode the beam intensity was an order of magnitude higher.

Fig.8 shows the raw TOF spectrum (at 0°) for a nominal beam energy of 61 MeV (11.2 MeV neutron energy). The flat background stems from the beam interaction with the target structure and can be subtracted with the help of a "gas-out" run. Using a windowless gas target [13] will allow a background-free operation.

3.3.2.4 $^{1}H(^{13}C,n_0)^{13}N$

This reaction gives kinematically collimated monoenergetic neutrons between 2.791 and 12.175 MeV. Beyond the latter energy neutrons from the $n+p+^{12}C$ exit channel will produce a break-up spectrum. The yield curve looks very promising especially at its maximum at 9 MeV (see 4.2.).

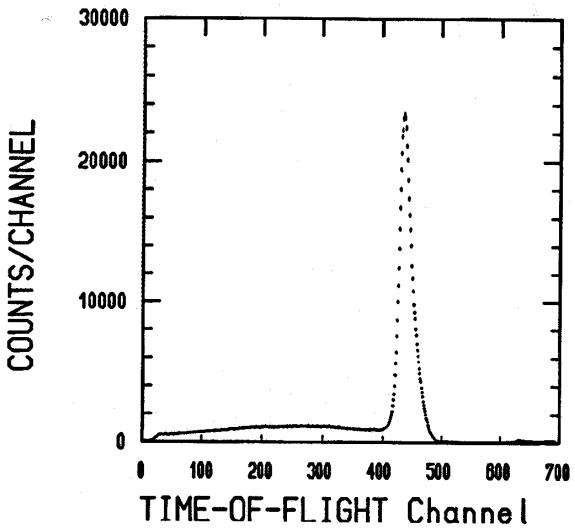

Fig.8. Neutron time-of-flight spectrum of the $^{1}H(^{11}B,n_0)^{11}C$ reaction at a nominal incident energy of 61 MeV. The neutron energy is 11.2 MeV.

3.3.2.4 $^{1}H(^{13}C,n_0)^{13}N$

This reaction gives kinematically collimated monoenergetic neutrons between 2.791 and 12.175 MeV. Beyond the latter energy neutrons from the $n+p+^{12}C$ exit channel will produce a break-up spectrum. The yield curve looks very promising especially at its maximum at 9 MeV (see 4.2.).

Measurements at Tohoku University [48] have been reported with a ^{13}C beam of 10 nA from a cyclotron at energies between 42.5 and 45.2 MeV producing neutrons between 3.6 and 5 MeV. After emptying the gas target the structural background was determined to be only a few % of the foreground. In addition, there were practically no gamma-rays connected with the source.

The observed yields were noticeably smaller than expected from $^{13}C(p,n_0)^{13}N$ data; near 5 MeV neutron energy by about a factor of two. So the predictions of the code DROSG-96 might be too optimistic for this reaction.

3.3.2.5 $^{1}H(^{15}N,n_0)^{15}0$

Monoenergetic neutrons between 3.318 and 25.726 MeV, kinematically collimated, can be generated with this reaction which provides the widest known monoenergetic range [49].

Compared with ^{11}B - ^{1}H the specific yield in the gap region is about a factor of 2 less. In addition, the abundance of ^{15}N is quite small and the required charged particle energy is higher. So ^{15}N - ^{1}H will be an interesting source only beyond 11.9 MeV where ^{11}B - ^{1}H becomes a two-(four-) line source. Up to now no measurement of the neutron output of this source has been reported.

3.3.3 (d,n) reactions

Because of the positive Q-value a smaller acceleration voltage is needed to get the desired neutron energy than with (p,n) reactions so that low voltage accelerators can produce high energy neutrons (14-MeV-generators!).

However, because the deuterons are loosely bound only, they break-up easily so that the monoenergetic energy range spans a few MeV at best (see Table 2).

In addition, deuteron beams require clean vacuum technique in the accelerators: carbon and oxygen contaminations (especially on the front face of the entrance window) will generate disturbing neutron background. Either cold traps in connection with oil diffusion pumps or oil free pumps (like mercury diffusion pumps) must be used.

3.3.3.1 $^{2}H(d,n)^{3}He$

This "work horse" of the traditional monoenergetic sources gives monoenergetic neutrons between 2.45 and 7.706 MeV. Because it is relatively easy to use (no radioactivity involved) it is applied even in the break-up region. Reliable additional data on the neutron background from break-up reactions was the backbone of a reevaluation [50]. Thus, the useful energy range of this popular source may be extended beyond 10 MeV neutron energy by applying calculated corrections for this background [51]. Besides, a procedure was advanced which describes the energy spectrum of the break-up neutrons (up to 12 MeV primary neutron energy [52]) analytically. However, above that energy this reaction is not at all a useful monoenergetic neutron source because of the extremely strong contamination with intrinsic break-up neutrons. On the contrary, this source has been used as a white neutron source [53].

The differential cross sections of d-D are the most accurate. Around 5 MeV they are known absolutely to about 1.5%. However, some more recent low energy data [54] are noticeable lower in scale and have a much stronger anisotropy than all previous data and the latest evaluation [4]. This evaluation is, on the other hand, supported by another set of more recent data [55].

The symmetry of the c.m. cross sections around 90° makes the d-D reaction a convenient tool for measuring the ratio of the detection efficiency at the corresponding pair of energies.

For neutron energies below about 5 MeV also solid (deuterated) targets are in use to give better energy resolution (no window), at the expense of intensity.

The p-T reaction is superior to d-D in nearly all aspects [9].

3.3.3.2 $^{3}H(d,n)^{4}He$

The monoenergetic range of this source extends from 14.03 to 20.461 MeV. Beyond the latter energy the usefulness of this source is limited by the strong rise of the break-up cross section with increasing incident deuteron energy. It is best known for neutron production at "14 MeV" by means of neutron generators, i.e. low energy deuteron accelerators in connection with solid tritiated targets [56,57].

Even at the resonance near 14 MeV the specific yield of this reaction is very meagre. When, as usual, solid targets are used it is further decreased by an order of magnitude. At low beam energies the energy of neutrons emitted at about 95° is practically independent of the projectile energy. Thus the specific yield is larger by an order of magnitude than that at 0° (where the neutron energy depends strongly on the beam energy).

The rather high room background because of the near-isotropy of the neutron emission is another drawback of this source. Some attention must be paid to the self-target build-up by implantation of deuterons into the target resulting in background neutrons from the d-D reaction. In spite of all these disadvantages up to now only this source reaction has been used in the design of intense monoenergetic neutron sources (see 4.4).

In recent years there have been several reevaluations of the differential cross sections. One was based on an R-matrix analysis which included unpublished $^{2}H(t,n)^{4}He$ differential cross section data [10]. It has resulted in pronounced changes, especially at back angles and at lower energies. (E.g. at 0.4 MeV the previously assumed isotropy does not hold. At 2 MeV the shape changed by as much as ±6.5% which was just about the estimated maximum shape uncertainty at this energy [5]. The maximum change in scale - 7.2% - occurred at 1.6 MeV.)

Another was an effort to provide differential cross sections up to 30 MeV deuteron energy requested for FENDL [58], by extrapolating from 19 MeV to 30 MeV [10]. Later an evaluation [11] using charge symmetric $^{3}He(d,p)^{4}He$ data [59 - 62] allowed an extension of the 0° cross section to 200 MeV neutron energy. These data are considerable higher than an old estimate and quite different in shape [27].

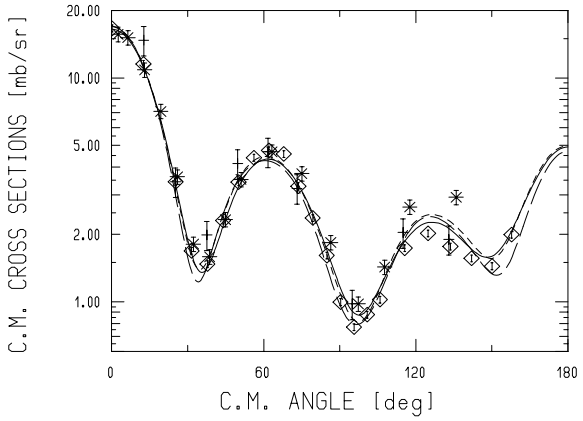

FIG. 9. Differential cross sections of d-T at 19.5 MeV. Diamonds are from [63], stars from [65] and crosses from [66].

Just recently new differential cross section data [63] became available which extend the energy range up to 19.5 MeV. The measured 0° excitation function agrees perfectly with that of the FENDL-evaluation [64] but differs somewhat from a later prediction [11] using charge symmetric ^{3}He(d, p)^{4}He data.

Fig. 9 shows the new differential cross section data at 19.5 MeV together with older data at 19 MeV [65,66]. The lines are the sol-utions of various evaluations using the old data. Obviously, these new data with a distinctly lower third maximum will contribute to a better pre-diction of the d-T cross sections around 20 MeV.

3.3.3.3 ^{15}N(d,n)^{16}O

Among the multi-line (d,n) reactions d-^{15}N has the highest separation energy (> 5.69 MeV, see Table 2). In addition, the lowest energy ground state neutron line is at 9.312 MeV (E_d=0 MeV), the lower edge of the "gap". The much higher Q-value of d-^{15}N than d-D (9.90 vs. 3.27 MeV) gives the former reaction two advantages. E.g. for the production of 12 MeV neutrons (the middle of the "gap") only 2.22 MeV deuterons are needed (instead of 8.92 MeV) allowing the utilization of low energy accelerators. In addition this energy is below the (d,n+p) break-up energy of 2.24 MeV resulting in a very low structural as well as room background. However, the intrinsic signal-to-background ratio of d-^{15}N at 12 MeV is about 1:4 [67] compared to is 1:1 for d-D [68]. Besides, the energy separation to the highest energy intrinsic background is 5.939 MeV vs. 6.473 MeV, only. Besides, the specific yield for neutron production is about 1000 times higher for d-D (see 4.2). So if one must produce 12 MeV neutrons with an accelerator that cannot provide 9.9 MeV d-^{15}N might be useful [69,70], despite the very low yield. Fig. 10 shows the neutron energy spectrum reported there.

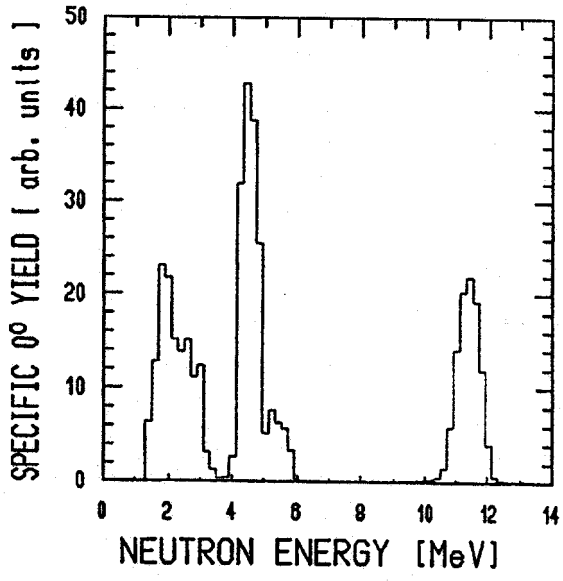

FIG. 10. Neutron energy spectrum of 11.4 MeV „monoenergetic“ neutron production by the reaction $^{15}N(d,n)^{16}O$ [67].

3.3.4 Inverse (d,n) reactions

3.3.4.1 $^{2}H(t,n)^{4}He$

The inverted d-T reaction gives monoenergetic neutrons between 14.03 and 23.006 MeV. The increased monoenergetic range is the result of the higher projectile energy required to give the same c.m. break-up energy. Although d-T and t-D have the same c.m. cross sections the total neutron output (integrated over solid angle) is 1.5 times higher in the t-D case (for the same c.m. energy spread). This results (at 90°) in a 1.5 times higher specific yield for t-D. The explanation is simple: for the same c.m. energy the triton energy is about 1.5 times higher than the deuteron energy which means that both projectiles have the same velocity and, therefore, the same specific energy loss in the target medium (a hydrogen isotope). Because of the higher energy of the tritons the relative loss is lower by a factor of 1.5 and consequently the specific yield higher by that factor. (Correspondingly the neutron output from t-H is three times that of p-T).

This source has been used at Los Alamos National Laboratory as an alternative to the d-T source for 14 MeV neutron production [40].

Information on the intrinsic break-up background of this source is sparse. At 16.4 MeV the background-to-signal ratio is reported to be about 100 [10]. For 20.22 MeV tritons completely stopped in deuterium [71] a factor of 30 was obtained. Double differential and differential (white) yields for the interaction of 20.22 MeV tritons with deuterium for angles between 0.3° and 75° are given there, showing a very strong forward peaking.

4. SELECTION GUIDE

4.1 Monoenergetic neutron production up to 100 keV

Production of monoenergetic neutrons of energies below 100 keV at 0° is possible with many (p,n) reactions by using proton energies just slightly above threshold (see Table 1). Usually, the cross sections are very small and consequently the yield is meagre. Unfortunately, the production of very low energy neutrons requires that the threshold

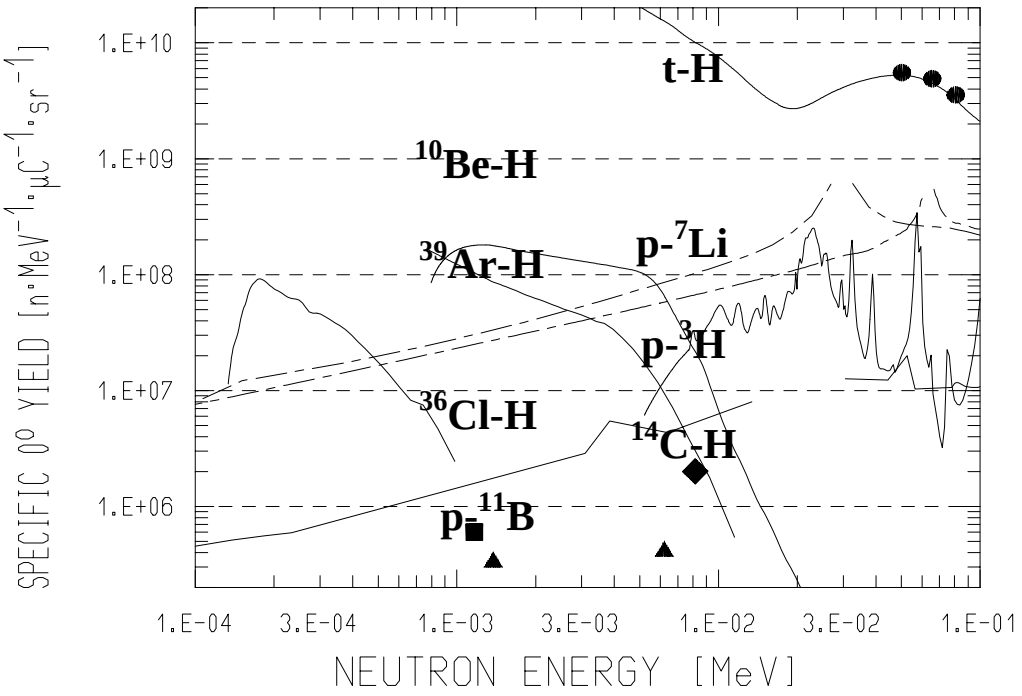

FIG. 11. Comparison of the specific neutron yield at 0° for two-body neutron production between 100 eV and 100 keV. The full dots indicate measurements of the t-H reaction, the full square is the resonance of ^{65}Cu(p,n), the full diamond one of ^{45}Sc(p,n) and the full triangles two of ^{59}Co(p,n).

energy is low and/or the mass of the target nucleus high. Both requirements result in a high specific energy loss of the proton, so that the neutron yield becomes low, even with high cross sections.

An alternate method takes advantage of the second, the low energy group from inverse (p,n) reactions (neutrons emitted at 180° in c.m.). Fig. 11 gives the specific 0° yield between 100 eV and 100 keV for 6 (p,n) reactions and 5 inverse (p,n) reactions. For p-^{45}Sc, p-^{59}Co and p-^{65}Cu the maximum of resonances are indicated by the full points.

Among the inverse reactions only t-H has been used for low energy neutron production (down to 50 keV [72]). The 3 dots on the curve show those energies, at which this reaction has been used as a neutron source.

At high enough projectile energies the neutron energy at 0° in inverse (p,n) reactions is approximately given by

$$E_n(0°) = m_1 \cdot Q^2 / (4E_1 \cdot m_H)$$

with E_n=neutron energy, E_1=projectile energy, m_1=projectile mass, Q=Q-value and m_H=proton mass.

From this formula the strong dependence on the Q-value can easily be seen. A search for (p,n) reactions with low Q-values and not too high mass numbers yielded p - ^{36}Cl, p - ^{39}Ar and p - ^{10}Be. As can be seen from Fig.11 the reaction ^{36}Cl-H can produce "monoenergetic" neutrons with energies as low as 100 eV. However, all inverse (p,n) reactions will always have a an additional high energy neutron group which could be detrimental.

Considering the intensity alone, t-H is better by at least an order of magnitude than any other reaction. The differential yield integrated from 5 keV to 40 keV into one steradian is 2.10^{11} neutrons per second and μA. However, the yield of the high energy group is 3000 times higher with an average neutron energy of nearly 31 MeV. In addition, there would be intrinsic and structural background.

From the (p,n) reactions shown in this graph p-^{45}Sc has been considered before [73]. The energy of the resonance is nearly optimal. However, the low yield of this reaction and the other (p,n) reactions with energies below 10 keV (p - ^{59}Co and p - ^{65}Cu) makes applications other than detector calibrations wearisome.

4.2 Monoenergetic neutron production between 100 keV and 20 MeV

Fig. 12 shows the energy dependence of the specific neutron yield at 0° for all sources considered here under the assumption of isotopically pure targets as calculated by DROSG-96. (Hydrided targets which are frequently used for d-T and p-T, and sometimes for d-D

would give about an order of magnitude less yield!) Thinner portions of the curves indicate the energy region with contamination by source-intrinsic background neutrons.

The outstanding feature is the overwhelming specific yield of the t-H reaction over all the energy range. This specific yield is more than 165 times higher than that of the well known resonance of d-T used in 14 MeV neutron generators.

In the region between 10 MeV and 14 MeV which is of special interest for fusion research there are, aside from t-H, three more monoenergetic sources to be considered: ^{11}B-^{1}H, ^{13}C-^{1}H and ^{15}N-^{1}H. The last reaction has not been tried out yet. ^{13}C-^{1}H has only been measured at 2 energies (2.7 MeV and 4.2 MeV [48]). So at present, only ^{11}B-^{1}H remains as alternative to t-H. However, its specific yield at the resonance near 11.4 MeV neutron energy is about a factor of 25 lower.

The two next best choices, d-^{11}B and d-^{7}Li have a somewhat higher yield but can - even at back angles - only provide neutrons with a minimum energy of 12.464 and 12.852, resp.. The reaction d-^{13}C is hampered by its small separation energy of about 2 MeV. Except for special applications, these two sources cannot really compete with the other four.

If the secondary neutrons of the break-up continuum do not disturb, also p-T or d-D may be used. Considering the specific yield alone they are about equivalent. However, when the target cell properties (entrance window!) are included p-T gives more yield by a factor of 2 than d-D [4]. Here, too, a windowless target [13] would be very beneficial especially in connection with d-D.

For energies below about 1 MeV p-^{7}Li is the usual choice. The main advantage is the availability of isotopically pure windowless targets.

A detailed comparison with emphasis on practical aspects of these sources (except for the (d,n) reactions with high Q-values) can be found elsewhere [9].

4.3 Monoenergetic neutron production above 20 MeV

Fig.13 summarizes the present status of monoenergetic neutron production above 20 MeV. As pointed out before (see 3.3.1.2) p-^{7}Li is the favorite source at high energies, despite the "contamination" with the neutrons from the excitation of the 0.429 MeV level of ^{7}Be.

Although p-T is noticeable better, the character of the target (gas, radioactive) prevents its general use. A new extrapolation of the ^{3}H(p,n)^{3}He cross section [10] resulted in a yield curve which is lower, up to a factor of two at 200 MeV. Such lower values are prompted by the data at 318 MeV [74].

The 0° yield curve of d-D above 50 MeV as given in Fig. 13 is about 10% lower than previously assumed [27]. This is of little relevance because d-D at higher energies is not a practical monoenergetic source (see 3.3.3.1).

The high energy yield curve of d-T is based on extrapolations using the charge symmetric $^{3}He(d,p)^{4}He$ cross sect-ions [11]. A new evaluation based on new data [63] is not expected to give dramatic changes. Any such changes are of little importance because d-T is not a useful monoenergetic source at higher energies due to the immense intrinsic background of break-up neutrons. Thus d-T is a useful "monoenergetic" neutron source under special circumstances only. As the neutron background from the deuteron break-up on tritium is strongly forward peaked the signal-to-background ratio is much more favorable around 45° (at the second maximum or the shoulder of the differential cross section) than at 0°. This advantage of the 45° position is offset by the fact that the meagre monoenergetic yield of this reaction is reduced even further (by a factor of about 5, see 3.3.3.2.).

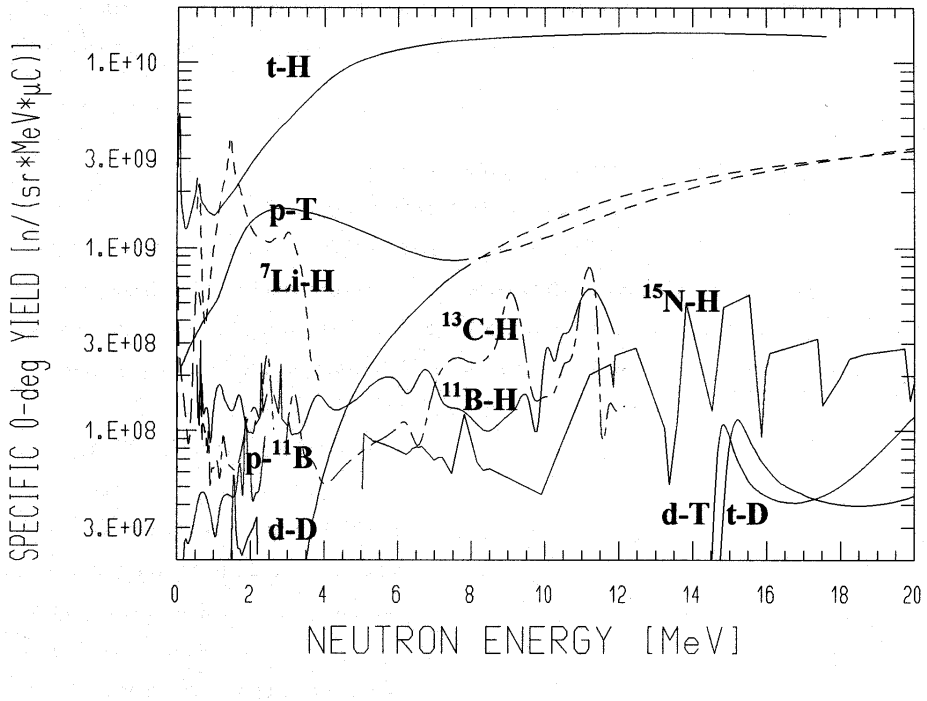

FIG. 12. Energy dependence of the specific neutron yield at 0° for the monoenergetic neutron sources considered in this paper. Dashed portions of the p-T and d-D curves indicate the energy region with contamination by source-intrinsic background neutrons.

4.4 INTENSE (MONOENERGETIC) SOURCES

4.4.1 General

In medical applications it is mandatory that one treatment is performed within a time span of much less than an hour, most other applications should last even shorter. Single shot experiments may last considerably longer. So a high yield from a neutron source is more important for applied purposes than in most experimental situations. In addition, neutron sources for scientific purposes are usually situated in special installations whereas applied sources should either be transportable or even portable [1,14]. So requirements for science oriented sources will often be less stringent than those for applied purposes. The development of such sources is just at the beginning so that the main emphasis here is laid on intense neutron source for scientific applications.

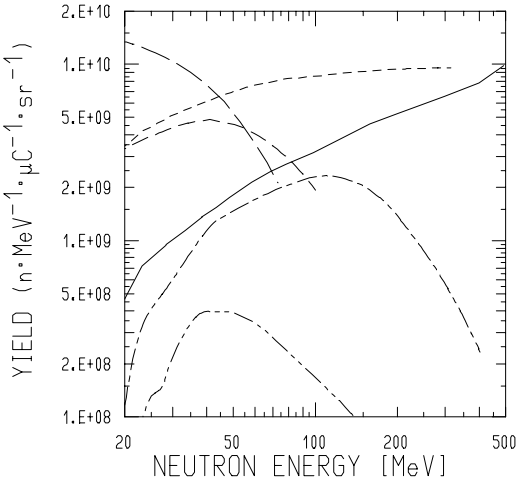

FIG. 13. Monoenergetic neutron production up to 500 MeV. From bottom to top: t-D, d-T, p-^{7}Li, d-D, p-T, t-^{1}H

4.4.1.1 Power considerations

Often the maximum neutron yield will be limited (at least theoretically) by the maximum power that may be dissipated in the target. Obviously there are media that can easily be cooled (liquids, in particular water), whereas others need auxiliary cooling media for the heat removal.

Under the assumption of equal target power the isotopic purity of the target (structure) is decisive because the energy loss in "structural" material does contribute to power but not to the (desired) yield. Obviously, an ideal target is isotopically pure and selfsupporting, i.e. it has neither entrance nor exit window.

Solid windowless targets for the hydrogen isotopes are, unfortunately not isotopically pure. Thus in such targets the yield is reduced by about an order of magnitude.

Liquid windowless targets can be realized by jets. For hydrogen targets of highest power a free standing water jet has been proposed [75] providing a 0.3 MW target for a d-D high intense neutron source. Similarly there was a proposal for a high- intensity 14-MeV cutoff neutron source based on the $^{1}H(t,n)^{3}He$ reaction [76].

Gaseous windowless hydrogen targets based on supersonic gas jets [19], [20], [21] have insufficient areal density so that a very high beam current is needed to compensate for it. However, the recent development of the plasma port hole [13] appears to be the solution for windowless gas targets of sufficient areal density.

4.4.2 14 MeV-neutron production

The only intense monoenergetic neutron sources presently available are those based on the d-T reaction using solid targets and supplying up to $3.5 \cdot 10^{13}$ "14" MeV neutrons per second [77]. Based on the specific yield alone, the best choice for a 14 MeV neutron source would be t-H.

Allowing a neutron energy width of 1 MeV the triton beam will be slowed down in the target from 20.98 to 19.65 MeV producing (at 0°) $1.4 \cdot 10^{10}$ n/(sr.μC) with an average energy of 14.1 MeV. With a current of 210 μA and an intrinsic target power of only 0.28 kW the same differential source intensity at 0° can be obtained as with 50 kW in the d-T case. Using a wider energy spread would reduce the required current rating of the accelerator. Thus, a comparison based on equal target power shows that the t-H reaction will produce about 200 times more neutrons into the forward direction than d-T, i.e. an equivalent source strength of about 10^{15} n/s appears feasible [9]. The status of this intense source has been described in detail [9] before the advent of the plasma port hole [13] which allows the construction of windowless gas targets. Thus an even higher neutron yield for the same power dissipation in the target should be obtainable.

Up to now the highest neutron intensity using the t-H reaction was obtained with a rotating target [43]. Using this target under the experimental condition given (10 μA beam current, gas cell 4.6 cm long with 1.1 MPa hydrogen gas, 25 μm of molybdenum entrance foil) a specific neutron intensity at 0° of $6.4 \cdot 10^{10}$ n $sr^{-1}s^{-1}$ could be obtained at a power of 0.22 kW. For an isotropic source this would correspond to $8 \cdot 10^{11}$n/s. As pointed out in the paper [43] this cell could withstand higher currents because of its thick entrance window. By using an exit window (again 25 μm Mo) and a bending magnet the target power would only be 0.02 kW.

4.4.3 SOURCES FOR FUSION MATERIAL TESTING

Candidate materials for various fusion reactor components must be tested under fusion-relevant neutron spectra and fluxes. For this purpose the International Fusion

Materials Irridation Facility has been planned, based on the (white) d-^{7}Li source reaction [78]. The alternative based on the monoenergetic t-H reaction [76] using a supersonic jet of ordinary water has several advantages

- a clean high energy cut-off at 14.6 MeV (much less high energetic contamination).
- comparatively simple target technology: a jet of water versus a jet of liquid lithium.

The addition of oxygen reduces the yield from hydrogen by about a factor of four because of the increased triton stopping power. On the other hand there are neutrons from the triton-oxygen interaction with a maximum energy beyond the triton energy (Q_{tO}=+1.268 MeV, whereas Q_{tH}=-0.764 MeV!). These neutrons are intrinsic background neutrons and, therefore, contaminate the monoenergetic spectrum. In a white spectrum obtained at 0° by stopping 20 MeV tritons in water the neutron yield from oxygen was 23 % of the hydrogen yield [79]. Using the t-H source with a water target at 0.3 MW a neutron yield at 0° of $5.5 \cdot 10^{14}$ n $sr^{-1}s^{-1}$ would be obtained (with an equivalent isotropic source strength of 7.10^{15} n s^{-1}). Into a total opening angle of 134° the total yield would be $4.3 \cdot 10^{14}$ n s^{-1} (with an equivalent isotropic source strength of $1.4 \cdot 10^{15}$ n s^{-1}).

Although this source, too, does not qualify as a monoenergetic source it appears to be the best choice for a high intense neutron source to be used in fusion material studies [76].

4.4.4 Sources for neutron radiotherapy

To minimize side effects in healthy tissue such neutron sources should have a low energy cut-off at about 10 MeV. Therefore, white sources do not really qualify but have been used because nothing better was available.

There are three target designs for use in radiotherapy based on d-D (as a white source). At Heidelberg [53] 100 μA of 10.6 MeV deuterons from a cyclotron were stopped in a 30 cm long target filled with 11 atm of deuterium. The window was 10 mg/cm² of Havar. The power of 1.1 kW was removed by cooling the cell with water and by circulating the cooled gas. To increase the life of the entrance foil the returning cool gas was directed at this foil to reduce the local heating. The typical life of the window was 600 μAh. A foil change could be performed within 5 minutes.

A higher areal density is obtained in a similar target with cryogenic cooling [80]. The target is cooled by circulation of the gas in a closed loop between the target and an external heat exchanger which is immersed in liquid nitrogen. The design goal was to stop 180 μA of 8.3 MeV deuterons in the 7.5 cm long gas cell (filled with deuterium of 10 atm at 80 K, with a Havar entrance foil of 10 mg/cm²). The cryogenic cooling does not only increase the areal density by nearly a factor of four but increases the tensile strength of Havar considerably [80].

Finally, a deuterium gas cell with a pressure rating of 33 atm has been reported [81] which was used with a 21 MeV deuteron beam of 2 μA.

As has been pointed out before [82] the t-H reaction gives an optimum spectrum for neutron radiotherapy because of the possibility of a low energy cut-off. With the advent of the plasma porthole [13] which would minimize undesired lower energy neutron background the situation has become even more favorable. Fig. 14 gives a realistic neutron energy spectrum for such an arrangement. Using a gaseous target with massfree entrance and exit windows does not only avoid structural background but reduces the dissipated target power as well. With proven heat removal technology [53] a target power of 1 kW would result in a clean thick target yield for neutrons between 10 and 14 MeV with differential neutron source intensities of $1.1 \cdot 10^{13}$ n $sr^{-1}s^{-1}$, corresponding to a (isotropic) source strength of $1.4 \cdot 10^{14}$ n/s.

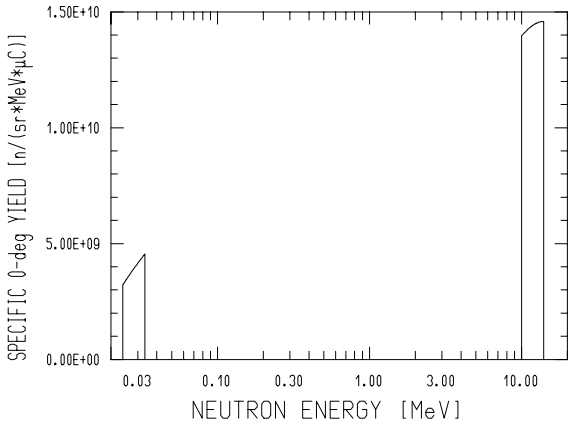

FIG. 14. Neutron energy spectrum from t-H with a sharp energy cutoff at 10 MeV.

4.4.5 Sources for fast neutron radiography

In recent years there has been not only an increase in quantity but also in quality of neutron radiography resulting in improved penetrabilty and selectivity. Good penetrability requires neutrons of high enough energies (of the order of 10 MeV). Even high energetic white sources have been tried [83].

Selectivity can be obtained by resonance radiography if the cross section of the isotope of interest peaks within the energy width of the source neutrons. In cases which require fast action (e.g. conveyor belts in mining operations) intense fast neutron sources with energy selection are needed. Although the t-H source would be best because of its high yield alternate intense monoenergetic sources must be considered if triton beams cannot be provided. In this case d-D is an obvious candidate.As pointed out in the previous section, d-

D targets with kW target powers have been designed for neutron radiotherapy [53],[80]. However, the deuteron break-up (Q=-2.2246 MeV) does not allow a clean monoenergetic source. To achieve clean conditions, two provisions are necessary [11]

a) background elimination by subtracting a neutron radiograph taken with the background neutrons, and
b) keeping the background small.

As described before [11] such an arrangement could consist of two gas cells as neutron targets between which the deuteron beam is swept at a rate appropriate to the problem. The background cell contains hydrogen gas instead of deuterium to simulate the energy loss of the deuteron beam. The break-up threshold for d-H is 6.674 MeV vs. 4.450 MeV for d-D. So, e.g. for monoenergetic neutrons of 8.3 MeV the net neutron spectrum will be contaminated with d-D break-up neutrons with a maximum energy of 1.623 MeV having an intensity close to 1% of the monoenergetic intensity.To make the structural background small, helium gas can be used as beam stop material, because the d-He break-up threshold is 3.345 MeV and there is no two-body neutron production by this reaction below 6.300 MeV. Such an arrangement could provide fast neutrons for resonant neutron radiography for energies up to at least 10 MeV. At this energy the uncorrectable background (from d-D break-up) will be about 25%.

5. CONCLUSIONS

There has been no evidence up to now that the cross section data bases used in the code DROSG-96 do not suffice today's applied needs. This is true specifically for the four "working horses" $^{3}H(p,n)^{3}He$, $^{7}Li(p,n_0)^{7}Be$, $^{2}H(d,n)^{3}He$ and $^{3}H(d,n)^{4}He$, even if some new data have become available:

- the data base of $^{3}H(p,n)^{3}He$ below 2.9 MeV could be improved through excellent new integrated data together with an independent R-matrix analysis of the ^{4}He-system,

- $^{3}H(d,n)^{4}He$ data near 20 MeV will be a valuable input for an evaluation at higher energies improving the data base near and above 20 MeV, however, attempts to improve the lower energy data base of the reaction $^{7}Li(p,n_0)^{7}Be$ which is of special interest in connection with BNCT failed insofar as the quality of the new data does not suffice.

Thick target yield curves in the double-valued energy region are tricky because their shape is dependent on the acceptance angle of the detector and on microscopic angle changeing effects (beam straggling, nuclear scattering).

An intense neutron source for resonant neutron radiography based on the d-D reaction offers both high intensity and a rather clean monoenergetic neutron beam. It should allow

the application of neutron radiography in areas that are not accessible otherwise. $^{1}H(t,n)^{3}He$ is *the* superior monoenergetic neutron source reaction in many respects:

- at 0° neutrons between 19.1 keV and 17.64 MeV can be produced with the highest specific yield of all sources over practically all the energy range.
- In the tens-of-keV range it is a convenient source for detector calibrations because its intensity can be calculated reliably.
- In the "gap" region (10 to 14 MeV) it surpasses its only competitor $^{1}H(^{11}B,n_0)^{11}C$ in specific yield by more than an order of magnitude.
- As a high intense neutron source for fusion material testing it offers attractive advantages over the competitor d-Li.
- For monoenergetic 14 MeV neutron production it surpasses the d-T based high intense RTNS-II source [77] (with a maximum source strength of $3.5 \cdot 10^{13}$ n/s at 50 kW) powerwise by more than two orders of magnitude. Of course, the accelerator design for t-H would be much more demanding.

REFERENCES

[1] SVED, J., The First IEC Fusion Industrial Neutron Generator and Developments, Proceedings of the Fifteenth International Conference on Applications of Accelerators in Research and Industry, Denton Texas, (1998) p. 704

[2] BROLLEY, J. E., Jr., and FOWLER, J. L. Fast Neutron Physics, **Vol. I**, (J. B. MARION and J. L. FOWLER, Eds.), Interscience, New York (1960) p.73

[3] UTTLEY, C. A., Sources of monoenergetic neutrons, Neutron Sources for Basic Physics and Applications (S. CIERJACKS, Ed.), Pergamon Press, Oxford (1983) p.19

[4] DROSG, M., SCHWERER, O., Production of Monoenergetic Neutrons between 0.1 and 23 MeV: Neutron Energies and Cross Sections, Handbook on Nuclear Activation Data, K. Okamoto, Ed., IAEA Tech. Report Ser. 273, Vienna 1987.

[5] DROSG, M., Production of Fast Neutrons with Targets of the Hydrogen Isotopes. Source Properties and Evaluation Status of the Cross Sections, Int. Atomic Energy Agency Report IAEA-TECDOC-410 (1987) (Proc. IAEA Adv. Group Meeting on Neutron Source Properties, Leningrad, June 1986) p.239

[6] DROSG, M., Updating Survey of Some Less Common Fast Neutron Sources: $^{9}Be(p,n)^{9}B$, $^{11}B(p,n)^{11}C$, $^{51}V(p,n)^{51}Cr$ and $^{9}Be(O,n)^{12}C$, Int.Atomic Energy Agency Report IAEA-TECDOC-410 (1987) (Proc. IAEA Adv. Group Meeting on Neutron Source Properties, Leningrad, June 1986) p. 285

[7] DROSG, M., Properties of Monoenergetic Neutron Sources from Proton Reaction with Nuclei other than Tritons, Proc. IAEA Consultants' Meeting on Neutron Source Properties, Debrecen 1980, K. Okamoto, Ed., IAEA/Int. Nucl. Data Comm. Report INDC(NDS)-114/GT (1980) p. 241

[8] DROSG, M., Production of Fast Monoenergetic Neutrons by Charged Particle Reactions Among the Hydrogen Isotopes. Source Properties, Experimental Techniques and Limitations of the Data, Proceedings IAEA Consultants' Meeting on

Neutron Source Properties, Debrecen 1980, K. Okamoto, Ed., IAEA/Int. Nucl. Data Comm. Report INDC(NDS)-114/GT (1980). p. 201

[9] DROSG, M., Sources of Variable Energy Monoenergetic Neutrons for Fusion Related Applications, Nucl. Sci. Eng. **106**, 279 (1990)

[10] DROSG, M., Sources of fast monoenergetic neutrons. More recent developments, in Neutrons and their applications, (VOURVOPOULOS, G., and PARADELLIS, T. Ed.), Proc. SPIE **2339**, 145 (1995).

[11] DROSG, M., Monoenergetic neutrons in the energy range from 100 eV to 200 MeV from two-body reactions with the hydrogen nuclei, Proc. 5th International Conf. on Applications of Nucl. Techniques Neutrons in Research and Industry, Sissi, Crete, June 1996, Proc. SPIE **2867**, 490 (1997)

[12] VOURVOPOULOS, G., and PARADELLIS, T. (Eds.), Neutrons and their applications, International Conference, Proc. SPIE **2339** (1995).

[13] GERBER, W., LANZA, R. C., HERSHCOVITCH, STEFAN, A., CASTLE, P., C. and JOHNSON, E., The Plasma Porthole: a Windowless Vacuum-Pressure Interface With Various Accelerator Applications by Gerber, Proceeding of the 1998 Denton Conference, preprint as a priv. communication by LANZA, R. C., 1999.

[14] REICHARDT, J.W., MF Physics Corporation, Portable Pulsed Neutron Generator Specifications Private Communication (1999).

[15] ALLEN, B.J., Neutrons in cancer therapy, in Neutrons and their applications, VOURVOPOULOS, G., and PARADELLIS, T. (Eds.), Proc. SPIE **2339**, 494 (1995).

[16] SOLEILHAC, M., Production de neutrons monocinétiques jusqu'à 20 MeV avec des accélérateurs du type Van de Graaff, Centre d'Etude de Bruyères-le-Chatel, Report CEA-N-1812, July 1975.

[17] DROSG, M., DROSG-96, PC database for 33 neutron source reactions, documented in the IAEA report IAEA-NDS-87 Rev. 4 (March 1997).

[18] DROSG, M., Angular Dependences of Neutron Energies and Cross Sections for 11 Monoenergetic Neutron Source Reactions, Computer-Code DROSG-87: Neutron Source Reactions (O. Schwerer, ed.) Documentation Series, Nuclear Data Section, October 1987.

[19] BECKER, H. W., BUCHMANN, L., GÖRRES, J., KETTNER, K.U., KRÄWINKEL, H., ROLFS, C., SCHMALBROCK, P., TRAUTVETTER, H. P. and VLIEKS A., Nucl. Instrum. Meth., **198**, (1982) 277

[20] ARMSTRONG, D. D., EMIGH, C. R., MEIER, K. L., MEYER, E. A., and SCHNEIDER, J. D., Nucl. Instr. Meth., **145**, (1977) 127

[21] DELEEUW, J. H., HAASZ, A. A., and STANGEBY, P. C., Nucl. Instr. Meth., **145**, (1977) 119

[22] AUDI, G. and WAPSTRA, A.H., "The 1995 update to the atomic mass evaluation", Nuclear Physics **A595**, (1995) 409

[23] ZIEGLER, J. F., ed., The Stopping and Ranges of Ions in Matter, **Vol. 3** HYDROGEN, Stopping Powers and Ranges in All Elements, **Vol. 5**, Heavy Ions, Stopping Powers and Ranges, Pergamon, 1977, 1980.

[24] KONONOV, W.I., POLETAEV, E.D., JURLOV, B.D., At. Energija **43**, (1977) 303

[25] LEE, C. L. and ZHOU, X.-L., Nucl. Inst. Meth. Phys. Res. **B152**, (1999) 1
[26] DROSG, M., McDANIELS, D.K., HOPKINS, J.C., SEAGRAVE, J.D., SHERMAN, R.H. and KERR, E.C., Physical Review **C9**, (1974) 179
[27] RAPAPORT, J., Radiation Effects **92-96**, (1986). 1229
[28] SIMAKOV, S. P., LOVCHIKOVA, G. N.,. TRUFANOV, A. M, VINOGRADOV, V. A. and KOBOZEV, M. G., Nonmonoenergecity of neutron source based on the solid tritium target, XIV Int. Workshop on Nucl. Fission Physics, Obninsk (Russia) 12 - 15 Oct 1998.
[29] BRUNE, C. R., HAHN, K. I., KAVANAGH, R. W. and WREAN, P. R., Total cross section of the $^{3}H(p,n)^{3}He$ reaction from threshold to 4.5 MeV, priv. communication from Brune by way of a preprint (1999)
[30] HALE, G. M., priv. communication (1999)
[31] WILBURN, W. S., HUFFMAN, P. R., ROBERSON, N. R., TORNOW, W., GOULD, C. R., KEITH, C. D. and HALE, G. M., Few Body Systems **24**, (1998) 27
[32] DROSG, M.: The $^{3}H(p,n)^{3}He$ Differential Cross Sections Below 5 MeV and the n-^{3}He Cross Sections, LA-8215-MS, LASL (1980)

[33] LISKIEN, H. and PAULSEN, A., At. Data Nucl. Data Tables **15**, (1975) 57
[34] MEADOWS, J. W. and SMITH, D. L., Neutrons from proton bombardment of natural Lithium, Argonne National Lab., IL, Report ANL-7938 (1972).
[35] MEADOWS, J. W. and SMITH, D. L., Neutron source investigations in support of the cross section program at the Argonne fast neutron generator, Argonne National Lab., IL, Report ANL/NDM-53 (1980)
[36] MEADOWS, J. W., Determination of the energy scale for neutron cross section measurements employing a monoenergetic accelerator, Argonne National Lab., IL, Report ANL/NDM-25 (1977)
[37] HARKER, Y. D., HARMON, F., SEAMANS. J., Jr., SERRANO, S., TRAMMELL, W., YOST, L., ZHOU, X.-L. and HAMM, R., Accelerator neutron sources for neutron capture therapy using near threshold charged particle reactions, Proc. 5th International Conf. on Applications of Nucl. Techniques, Neutrons in Research and Industry, Sissi, Crete, June 1996, Proc. SPIE **2867**, (1997) 80
[38] HARKER, Y. D., priv. communication (1999)
[39] DESIMONE, D. J., KEGEL, G. H. R., EGAN, JJ., BERTONE, P.and STAPLES, P., Nucl.Inst.Meth. Phys.Res. **A388**, (1997) 443
[40] DRAKE, D. M., AUCHAMPAUGH, G. F., ARTHUR, E. D., RAGAN, C. E., and YOUNG, P. G., Nucl. Sci. Eng., **63**, (1977) 401
[41] LISOWSKI, P. W., AUCHAMPAUGH, G. F., DRAKE, D. M., DROSG, M., HAOUAT, G., HILL, N.W., NILSSON, L., Cross Sections for Neutron-Induced, Neutron Producing Reactions in ^{6}Li and ^{7}Li at 5.96 and 9.83 MeV, Los Alamos Sci. Lab., Report LA-8342 (1980)
[42] DROSG, M., LISOWSKI, P.W., HARDEKOPF, R.A., DRAKE, D.M., MUELLNER, M., Cross Sections for Neutron-Producing Reactions Induced by 6 and 10 MeV Neutrons Incident on ^{10}B and ^{11}B", Los Alamos Nat. Lab., Report LA-10665-MS, (May 1986)

[43] HAIGHT, R. C. and GARIBALDI, J., A Rotating Gas Cell for High Intensity Mono-energetic Neutron Production, Nucl. Sci. Eng., **106**, (1990) 296
[44] DROSG, M.,. DRAKE, D. M and MAZARIK, J., Nucl. Inst. Meth. Phys. Res. **B94**, (1994) 319
[45] DROSG, M., The $^{1}H(^{7}Li,n)^{7}Be$ Reaction as a Neutron Source in the MeV Range, Los Alamos Scientific Lab., Report LA-8842-MS (1981)
[46] DAVE,J. H., GOULD, C. R., WENDER, S. A., SHAFROTH, S. M., Nucl. Instrum. Methods Phys. Res. **200**, (1982) 285
[47] CHIBA, S., MIZUMOTO, M., HASEGAWA, K., YAMANOUTI, Y., SUGIMOTO, M., WATANABE, Y., and DROSG, M., The $^{1}H(^{11}B,n)^{11}C$ Reaction as a Practical Low Background Monoenergetic Neutron Source in the 10 MeV Region, Nucl. Instr. Meth. Phys. Res. **A281**, (1989) 581
[48] HASEGAWA, K., KOTAJIMA, K., KITAMURA, M., YAMAYA, T., SATOH, O., ASHINOZUKA, T., and FUJIOKA, M., Production of Focused Neutron Beam Using Heavy Ion Reaction, Proc. 11th Int. Conf. on Cyclotrons and their Applications, Tokyo, 1987. p. 642
[49] DROSG, M.., Novel Monoenergetic Neutron Sources for Energies Between 2.5 and 25.7 MeV, Nucl. Inst. Meth. Phys. Res. **A254**, (1987) 466
[50] CABRAL, S., BOERKER, G., KLEIN, H. and MANNHART, W., Nucl. Sci. Eng. **106**, (1990) 308
[51] SMITH, D. L., MEADOWS, J. W., Method of neutron activation cross section measurement for E_n=5.5-10 MeV using the D(d,n)He-3 reaction as a neutron source, Argonne National Lab., IL, Report ANL/NDM-9 (1974).
[52] KORNILOV, N. V., Possibilities of Experimental Determination and Theoretical Prediction of Different Properties of Accelerator Based Neutron Sources, p. 230, Int. Atomic Energy Agency Report IAEA-TECDOC-410 (1987) (Proc. IAEA Adv. Group Meeting on Source Properties, Leningrad, June 1986)
[53] SCHRAUBE, H., MORHART, A., AND GRUENAUER F., Neutron and gamma radiation field of a deuterium gas target on a compact cyclotron, Proceeding of the 2-nd Symposium on Neutron Dosimetry in Biology and Medicine, Neuherberg, Sept. 30-Oct. 4, 1974, EUR 5273 (1975) 979-1001
[54] KRAUSS, A., BECKER, H. W., TRAUTVETTER, H. P., ROLFS, C., and BRAND, K., Nucl. Phys., **A465**, (1987) 150
[55] BROWN, R. E. and JARMIE, N., Differential Cross Sections at Low Energies for $^{2}H(d,p)^{3}H$ and $^{2}H(d,n)^{3}He$, LANL preprint LA-UR-89-953 (1989)
[56] CSIKAI, J., Production of 14 MeV neutrons by low voltage accelerators, Proc. Consultants Meeting on Neutron Source Porperties, Debrecen 1980 (K. OKAMOTO, Ed.), IAEA/Int. Nucl. Data Comm. Report INDC (NDS)-114/GT (1980) p.265
[57] BARSCHALL, H. H., 14 MeV D-T sources, Neutron Sources for Basic Physics and Applications (S. CIERJACKS, Ed.), Pergamon Press, Oxford (1983) p.57
[58] DUNFORD, C. L., priv. communication on the Fusion Evaluated Nuclear Data Library (FENDL), 1994.
[59] GAGLIARDI, C. A., and BETKER, A. C., Nucl.Instr.Meth.Phys.Res. **A284**, (1989) 356

[60] ROY, R., SEILER, F., CONZETT, H. E., and RAD, F. N., Phys. Rev. C, **24,** (1981) 2421
[61] KING, T.R., and SMYTHE, R., Nucl.Phys. **A183**, (1972) 657
[62] BERNAS, M., BACHELIER, D., LEE, J.K., RADVANYI, P., ROY-STEPHAN, M., BRISSAUD, I. and DETRAZ, C., Nucl.Phys. **A156**, (1970) 289
[63] TANG, H., ZHOU, Z., QI, B., ZHOU, C., DU, Y., XIA, H., WALTER, R. L., HOWELL, C. R., TORNOW, W., BRAUN, R. T., CHEN, ZE., CHEN, ZH. and CHEN, Y., Excitation function and angular distributions of the ^{3}H(d,n)^{4}He reaction in the energy range 6 to 23 MeV, INPC '95: International nuclear physics conference, Beijing (China) 21 - 26 Aug 1995, and priv. commun. (1999).
[64] HALE, G. and DROSG, M.., d-t reaction evaluation, Charged-particle library for FENDL/C-2.0, Version 1.0 March 1997.
[65] VLASOV, N. A., BOGDANOV, G. F., KALININ, S. P., RYBAKOV, B. V. and SIDOROV, V. A., Investigations of reactions of 18-MeV deuterons with light nuclei by the time-of-flight method, Int. Conf. Neutron Interactions with the Nucleus, Columbia Univ., N.Y., USA, report TID-7547 (1957) (W. W. Havens, Jr., Ed.)
[66] SIMMONS, J. E. and MALANIFY, J. J., Bull. Am. Phys. Soc. **13**, (1968) 564 and priv. communication from J. J. MALANIFY (1977).
[67] MATSUYAMA, S., SODA, D., BABA, M., OHKUBA, T., and HIRAKAWA, N., Application of ^{15}N(d,n)^{16}O neutron source for neutron scattering cross section measurements, Proc.Int.Conf. on Nucl.Data for Sci. and Technol., Gatlinburg, 1994.
[68] DROSG, M., AUCHAMPAUGH, G.F., Signal-to-Background Ratio for Neutron Production Between 10 and 14 MeV by the Reactions ^{3}H(p,n)^{3}He, ^{1}H(t,n)^{3}He, and ^{2}H(d,n)^{3}He, Nucl.Instr.Meth. **140**, (1977) 515
[69] MATSUYAMA, I., BABA, M., MATSUYAMA, S., KIYOSUMI, T., SANAMI, T., HIRAKAWA, N., ITO, N., CHIBA, S., FUKAHORI, T., MIZUMOTO, M., HASEGAWA, K., and MEIGO, S., Measurements of double-differential alpha-particle production cross sections using a gridded ionization chamber, Proc. 1993 Symposium on Nuclear Data, (KAWAI, M. and FUKAHORI, T., Eds.), JAERI-M 94-019 (1994).
[70] MATSUYAMA, S., SODA, D., BABA, M., IBARAKI, M., NAUCHI, Y., IWASAKI, S., and HIRAKAWA, N., Measurements of double-differential neutron emission cross sections of Fe and Nb for 11.5 MeV neutrons, Proc. 1994 Symposium on Nuclear Data, (KAWAI, M. and FUKAHORI, T., Eds.), JAERI-Conf 95-008 (1995).
[71] DROSG, M.., DRAKE, D.M.,. HAIGHT, R.C, NELSON, R.O., Fast neutron yield from 20-MeV tritons on water. Part II. Triton interaction with heavy water, Nucl. Instr. Meth. Phys. Res. **B73**, (1993) 392
[72] DROSG, M.., DRAKE, D.M. and MASARIK. J., Nucl.Inst.Meth.Phys.Res. **B94**, (1994) 319
[73] McMICHAEL, G.E., YULE, T.J., ZHOU, X.-L., Nucl.Instr.Meth.Phys.Res. **B99**, (1995) 847
[74] BLINOV, A. V., et al., J. Phys. G. Nucl. Phys. **8**, (1982) 223
[75] LOGAN, C. M., ANDERSON, J. D., BARSCHALL, H. H., and DAVIS, J. C., A Heavy Water Jet Target and a Beryllium Target for Production of Fast Neutrons,

Conf. on Radiation Test Facilities for the CTR Surface and Materials Program, P. J. PERSIANI (ed.), ANL/CTR-75-4 and UCRL-76858 (1975) p. 410

[76] CIERJACKS, S., HINO, Y., DROSG, M., Proposal of a High Intensity 14- MeV-Cut-Off Neutron Source Based on the $^{1}H(t,n)^{3}He$ Source Reaction, Nucl. Sci. Eng. **106**, (1990) 183

[77] DAVIS, J. C., RTNS-II: Experience at 14 MeV Source Strengths Between $1x10^{13}$ and $4x10^{13}$ n/s, Int. Atomic Energy Agency Report IAEA-TECDOC-410 (1987) (Proc. IAEA Adv. Group Meeting on Source Properties, Leningrad, June 1986) p. 303

[78] LAWRENCE, G. P., VARSAMIS, G. L., KRAKOWSKI, R. A., BHATIA, T. S., NEUSCHAEFER, G. H., SCHNURR, N. M., and BLIND, B., High-Flux Accelerator-Based Neutron Source for Fusion Materials and Technology Testing, Report on the International Fusion Materials Irradiation Facility Evaluation Panel, San Diego, California, February 14-17, 1989, (VERBEEK, R., Ed.) International Energy Agency (1989) p.149

[79] DROSG, M., DRAKE, D.M., Fast neutron yield from 20-MeV tritons on water. Part I. Triton interaction with light water, Nucl. Instr. Meth. Phys. Res. **B73**, (1993) 387

[80] KUCHNIR, F. T., WATERMAN, F. M., FORSTHOFF, H., SKAGGS, L. S., VANDER AREND, P. C., and STOY, S., Design of a Cryogenic Deuterium Gas Target for Neutron Therapy, Proc. Conf. on Use of Small Accelerators in Research, Teaching and Industrial Applications, Dexton, U.K. Oct. 1976, CONF-761059, p.513

[81] WEAVER, K. A., EENMAA, J., BICHSEL, H., and WOOTON, P., Med. Phys. **6**, (1979) 193

[82] DROSG, M., Proposal of a Novel High Intense Neutron Source for Radiation Therapy, Z.Physik **A 298**, (1980) 297

[83] GAVRON, A., MORLEY, K., MORRIS, C., SEESTROM, S., ULLMANN, J., YATES, G., and ZUMBRO, J., High energy neutron radiography, Proc. 5th International Conf. on Applications of Nucl. Techniques, Neutrons in Research and Industry, Sissi, Crete, June 1996, Proc. SPIE **2867**, (1997) 326